# APPLIED ELEMENT METHOD FOR DYNAMIC LARGE DEFORMATION ANALYSIS OF STRUCTURES

Hatem TAGEL-DIN[1] and Kimiro MEGURO[2]

[1] Member of JSCE, Ph.D., Visiting Researcher, Institute of Industrial Science, The University of Tokyo
(4-6-1 Komaba, Meguro-ku, Tokyo 153-8505, Japan)
[2] Member of JSCE, Dr. Eng., Associate Professor, International Center for Disaster-Mitigation Engineering,
Institute of Industrial Science, The University of Tokyo (4-6-1 Komaba, Meguro-ku, Tokyo 153-8505, Japan)

A new extension of the Applied Element Method (AEM) for structural analysis is introduced. This paper deals with the large deformation of structures under dynamic loading condition. As no geometric stiffness matrix is adopted, the formulation used for large deformation is simple and it can be applied for any structural configuration or material type. A new technique based on determining the residual forces due to geometrical changes is proposed. The accuracy of this technique is verified in small deformation range by eigen value analysis. In large deformation range, the collapse behavior of structures and the rigid body motion of the failed structural elements can be followed accurately.

*Key Words: Applied Element Method, AEM, large deformation, dynamic large deformation, eigen value analysis, rigid body motion*

## 1. INTRODUCTION

Applied Element Method (AEM) is a new method for structural analysis. The strongest point of the method is that total behavior of structures from small deformation up to collapse can be simulated with reliable accuracy. The accuracy of the method was verified in various publications. The structural behavior under static monotonic loading was introduced in Ref. 1). The internal stresses, strains, crack initiation, propagation and failure load could be calculated accurately[1]. In the method, the effect of Poisson's ratio could be considered using elements with three degrees of freedom[2]. The effect of crack opening and closing during cyclic loading was discussed in Refs. 1) and 3). It was shown that the newly developed method, AEM, is as accurate as the Finite Element Method (FEM) in small deformation range. The applicability of the method in large deformation range was also checked in case of elastic structures. It has been shown that highly nonlinear geometrical changes of the structure, including buckling loads, buckling modes and change of internal stresses due to buckling can be followed accurately[4].

In AEM, the structure is modeled as an assembly of small elements which are made by dividing the structure virtually, as shown in **Fig. 1 (a)**. Two elements shown in **Fig. 1** are assumed to be connected by a pairs of normal and shear springs set at contact locations which are distributed around the

element edges. Stresses and strains are defined based on the displacements of the spring end points. Three degrees of freedom are assumed for each element. For other details like calculation of spring stiffness, please refer Ref. 1). In case of reinforced concrete, the reinforcement bars and concrete are modeled as continuous springs connecting elements together. Concrete spring means the spring which is having the properties of concrete and steel spring means the spring having the properties of steel. When the stress calculated from forces acting on springs exceeds the critical principal stress, local failure of the elements is modeled by failure of springs connecting elements.

Although the AEM is much simpler in modeling than FEM, the analysis introduced in references (1) to (4) can be performed using the FEM also where the structure does not collapse. Extending the applicability of the methods like FEM and BEM to collapse analysis of structures is quite difficult. The main problem is the contradiction between the assumption that the media is a continuum and complicated fracture behavior of the structure during collapse. One of the few methods that can follow structure's behavior from zero load till total collapse is the Extended Distinct Element Method EDEM[5], [6]. This method can easily deal with the behavior in large deformation range accurately. However, the EDEM faces many difficulties like:

(a)     Element generation for AEM

(b)     Spring distribution and area of influence
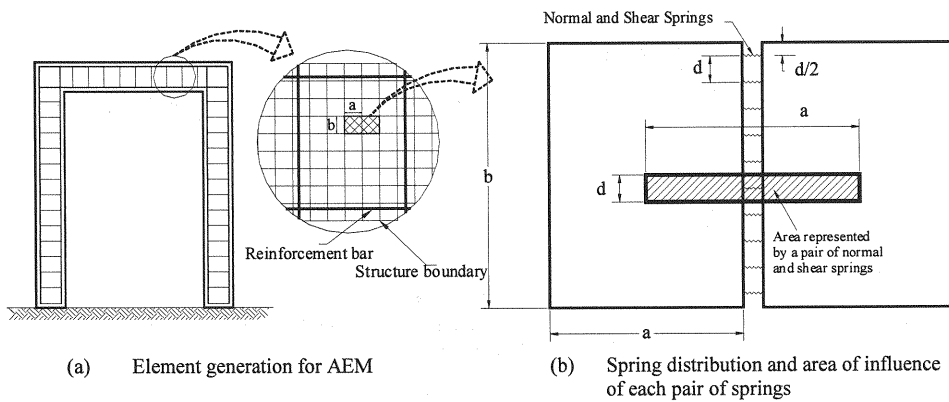         of each pair of springs

**Fig. 1**     Modeling of structure to AEM

1. Analysis under static loading condition is difficult.
2. The CPU time is long even in case of small deformation analysis and before cracking.
3. The time increment depends on the structural material and the element size. Simulation of materials of high stiffness composed of small-size elements leads to decreasing the time increment required and hence, the CPU time increases.
4. Although accuracy in discrete range is high, the accuracy in small deformation range is not as accurate as the FEM.

The main objective of this paper is to show that the collapse behavior, where both the material and geometry behave in highly nonlinear way, can be followed accurately.

## 2. ELEMENT FORMULATION IN DYNAMIC SMALL DEFORMATION RANGE

The general dynamic equation of motion in small deformation range is:

$$[M][\Delta\ddot{U}] + [C][\Delta\dot{U}] + [K][\Delta U] = \Delta f(t) - [M][\Delta\ddot{U}_G] \quad (1)$$

where $[M]$ is mass matrix; $[C]$ the damping matrix; $[K]$ the nonlinear stiffness matrix; $\Delta f(t)$ the incremental applied load vector; $[\Delta U]$ the incremental displacement vector; and $[\Delta\dot{U}]$, $[\Delta\ddot{U}]$ and $\Delta\ddot{U}_G$ the incremental velocity, acceleration and gravity acceleration vectors, respectively. Equation (1) is solved numerically using Newmark Beta technique[7].

**(1) Determination of mass matrix elements**

To simplify the dynamic problem and to reduce the size required for definition of mass matrix, the element mass and inertia are assumed lumped at the element centre. The mass matrix corresponding to an element, in case of square shaped elements, is:

$$\begin{bmatrix} M_1 \\ M_2 \\ M_3 \end{bmatrix} = \begin{bmatrix} D^2 \times t \times \rho \\ D^2 \times t \times \rho \\ D^4 \times t \times \rho / 6.0 \end{bmatrix} \quad (2)$$

where $D$ is the element size; $t$ the element thickness and $\rho$ the density of the material. It should be noticed that $[M_1]$ and $[M_2]$ are corresponding to the element mass in X and Y directions and $[M_3]$ corresponding to the element moment of inertia about the axis passing through centroid. Although the mass is lumped at the centroid of each element, its effect is very near to distributed mass systems if the element size is small.

The mass matrix is a diagonal positive definite matrix. This means that elements of the diagonal should be greater than zero. The mass matrix is very important in case of rigid body motion analysis. The static stiffness matrix becomes singular after failure due to cracking and separation of elements. This means that the matrix determinant reduces gradually till being zero at failure. Solution of a stiffness matrix having small value of determinant, ill-conditioned matrix[7], is generally inaccurate. This means that results obtained just before failure, or partial failure, of the structure is not accurate even if displacement control technique is used. This problem does not exist if the analysis is performed in dynamic case because addition of the mass matrix to the stiffness matrix results in a positive definite dynamic stiffness matrix even after failure.

Moreover, inertia forces play an important role in failure mechanism during collapse of the structure.

## (2) Determination of damping matrix

Sources of structural damping considered in the analysis of reinforced concrete:
1. Cracking of concrete.
2. Energy dissipation during loading and unloading process in compression springs, refer to **Sec. (4)**.
3. Unloading of reinforcement after yield.
4. Energy dissipation due to the process of crack closure and crack opening. When the crack is closed, shear stiffness is assumed to be equal to the initial stiffness. After reopening of cracks, shear forces developed during crack closure are redistributed, resulting in dissipation of shear energy stored during the crack closure.

The aforementioned damping sources affect the structural behavior in nonlinear stage only. The material damping matrix $[C]$ accounts for other sources of damping that are not considered above and its effect becomes dominant in elastic stage. The damping matrix calculated based on the first mode of deformation of the structure is as follows:

$$[C] = 2 \times \zeta \times w_1 \times [M] \qquad (3)$$

where $\zeta$ is the damping ratio and $w_1$ is the first natural frequency of the structure. The damping matrix values are determined using the eigen value analysis illustrated in the next section.
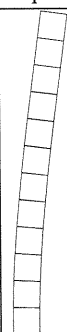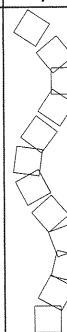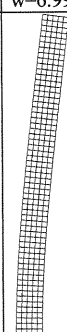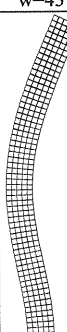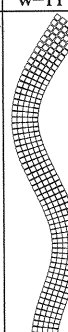
## (3) Eigen value analysis

Finding the vibration properties, natural modes and natural frequencies of a structure requires solution of the matrix eigen value problem. Moreover, making the analysis in frequency domain necessitates the previous knowledge of eigen values and eigen modes of the structure. The general equation for free vibration without damping is:

$$\left| w^2 [M] - [K] \right| [U] = 0 \qquad (4)$$

Although there are many techniques used for eigen value analysis, vector iteration with shifts technique[7], [8] is adopted in this study. This technique is a preferred method for eigen value analysis as it provides a practical tool for computing as many pairs of natural vibration frequencies and modes of a structure as desired.

Table 1 Eigen value analysis of a fixed base cantilever

| mode | 1st | 2nd | 3rd | 4th | 5th |
|------|-----|-----|-----|-----|-----|
| Case 1 |  | | | | |
| | w=6.99 | w=43 | w=117 | w=222 | w=350 |
| Case 2 |  | | | | |
| | w=6.53 | w=39.7 | w=106 | w=197 | w=306 |
| Theory* | w=6.46 | w=40 | w=113 | w=222 | w=367 |
| Error Case 1 | 8.00% | 7.00% | 4.00% | 0.00% | 5.00% |
| Error Case 2 | 1.00% | 1.00% | 6.00% | 11.00% | 16% |

*Shear deformations are not included*

## (4) Verification of eigen value analysis

The eigen value analysis results are compared with the theoretical values to verify the accuracy of the method. The natural frequencies and natural modes of the cantilever, shown in **Table 1**, are compared with the theoretical values[9]. To check the effect of element size, the analysis is performed for different element sizes, as shown in **Table 1**. The following can be concluded:
1. The obtained eigen values and eigen vectors are close to the theoretical results even in case of higher modes.
2. The values obtained using "12" elements are relatively close to those obtained by "300" elements especially in the first mode. This indicates that the method is numerically stable. The main reason for the difference is the change in the unsupported length in case of large element size.
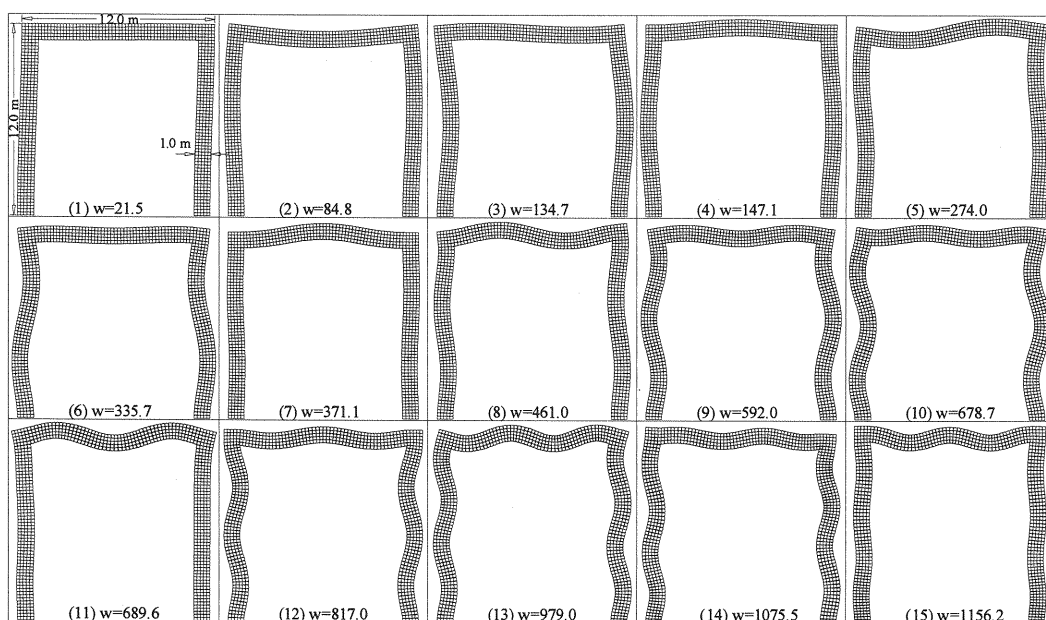
Fig. 2 Eigen value analysis of a fixed-fixed frame (modes and natural frequencies)

3. The difference between eigen values obtained through our method and theoretical values increases with higher modes. The reason is simply because the effects of axial and shear deformations, which are dominant in higher modes, are considered in our method, however, its effect is not included in the theoretical results.

**Figure 2** shows the results of eigen value analysis of a fixed-fixed frame. The frame thickness is assumed as 0.25 m; the Young's modulus as 2.1 x $10^7$ kN/m$^2$ and density as 2.5 t/m$^3$. The first fifteenth eigen modes and circular frequencies are shown in **Fig. 2**.

The above example shows that the new proposed method can be an efficient tool for structural analysis not only in time domain, but also in frequency domain. Obtaining accurate values of natural modes and natural frequencies is evidence that the method is applicable in frequency domain. However, as frequency domain analysis can not be applied to highly nonlinear material and geometrical behavior, which is the main target of this research, no examples are introduced for such cases.

## 3. ELEMENT FORMULATION IN DYNAMIC LARGE DEFORMATION RANGE

The consideration of large deformation in static loading condition was shown in Ref. 4). The analysis introduced in Ref. 4) was mainly for elastic materials under static loading condition. Analysis could be performed under load or displacement control. As collapse process of actual structures, especially concrete structures, is mainly a dynamic process, the method is extended to follow the large deformation behavior under dynamic loading condition. The general dynamic equation of motion in large deformation case is:

$$[M][\Delta \ddot{U}] + [C][\Delta \dot{U}] + [K][\Delta U] = \Delta f(t) + R_m + R_G \quad (5)$$

where $[M]$ is mass matrix; $[C]$ the damping matrix; $[K]$ the nonlinear stiffness matrix; $\Delta f(t)$ the incremental applied load vector; $[\Delta U]$ the incremental displacement vector; and $[\Delta \dot{U}]$ and $[\Delta \ddot{U}]$ the incremental velocity and acceleration vectors, respectively. Equation (5) simply represents the equilibrium equation between external applied loads and internal forces (internal stresses, inertia forces and damping forces). The terms "$R_m$" represent additional load vectors due to the nonlinear behavior of the material. After applying a small load increment, the structure geometry is modified and hence, incompatibility between external loads and other forces occurs. This results in the additional load vector "$R_G$". The main difference between the proposed method and the conventional methods is that the geometrical stiffness matrix is omitted and its effects were replaced by adding the geometrical changes effects as an "additional load vector $R_G$". This technique

was applied in Refs. 4) and 12) and results showed high accuracy.

The method is applied using the following steps:
1. Solve for gravity loads under static condition and get the internal forces.
2. Apply a load increment, $\Delta f(t)$.
3. Assume that $R_m$ and $R_G$ are zeros and solve Eq. (5) using Newmark Beta method[8] to get incremental displacement.
4. Calculate incremental strains and stresses.
5. Calculate incremental and total velocities and accelerations.
6. Modify the geometry of the structure according to the calculated incremental displacements by updating the location of elements.
7. Modify the direction of spring force vectors according to the new element configuration. Changing the direction of spring forces around elements leads to incompatibility between applied loads and internal stresses, damping forces and inertia forces.
8. From the calculated stresses, check the situation of cracking and calculate the material residual load vector $R_m$.
9. Calculate the element force vector from surrounding springs of each element, $F_m$.
10. Calculate the geometrical residuals around each element from Eq. (6)

$$R_G = f(t) - [M][\ddot{U}] - [C][\dot{U}] - F_m \qquad (6)$$

Equation (6) means that the geometrical residuals account for the incompatibility between external applied and internal forces, damping and inertia forces due to the geometrical changes during analysis. It should be noted that residual forces are calculated based on total stress value. Gravity forces are considered as an external applied force. Small deformations are assumed during each increment.
11. Calculate the stiffness matrix for the structure in the new configuration considering stiffness changes at each spring location due to cracking or yield of reinforcement.
12. Apply again a new load increment and repeat the whole procedure from step 2.
13. Material and geometrical residuals calculated from the previous increment can be incorporated in solution of Eq. (6) to reduce the time of calculation.

It should be also emphasized that this technique can be applied in both static and dynamic loading conditions. In case of static loading condition, the mass and damping matrices are set equal to zero.
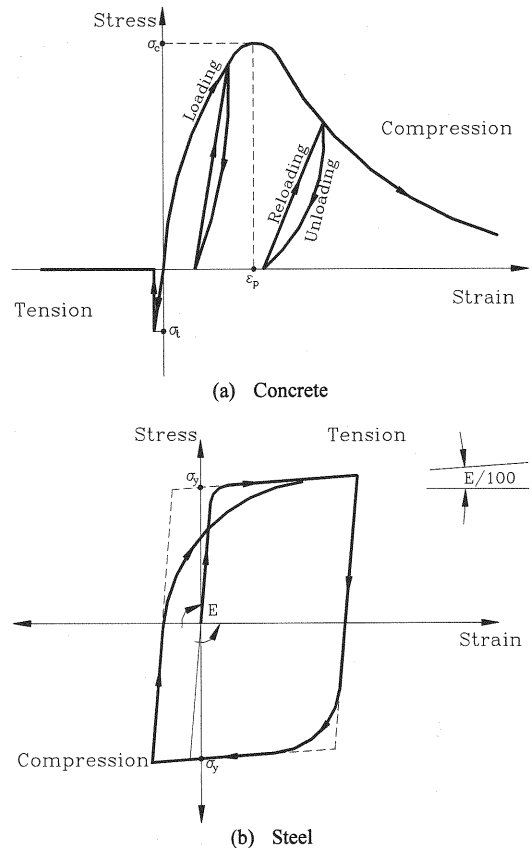


(a)  Concrete



(b)  Steel

Fig. 3 Material models for steel and concrete

The main limitation in static analysis is that separation of elements is not permitted during analysis as it makes the stiffness matrix singular. On the other hand, analyzing structures subjected to dynamic loading condition enables us to follow both geometrical changes of the structure and the rigid body motion during failure. As the deformations are assumed to be small in each load increment, small time increment should be used.

## 4.  MATERIAL MODELING

One of main difficulties in this kind of analysis is how to deal with compression crushing of elements. Having crushing of elements at the support location means, from numerical view point, that the elements lose all its stiffness and the structure is not connected to the ground any more. In this analysis, Maekawa compression model[10] is adopted till 1% strain in compression. This model is shown in **Fig. 3 (a)**. After reaching this strain, minimum stiffness value (0.01 of the initial value) is assumed so that the connection of the element to the other element is not lost. For reinforcement, the model shown in **Fig.**

**3 (b)**[11] is adopted. Namely after reaching 10% tensile strain, it is assumed that the reinforcement bar is cut. The force carried by the reinforcement bar is redistributed, when it reaches the failure criterion, by applying the redistributed force to the corresponding elements in the reverse direction. For cracking criteria, principal stress based failure criteria is adopted. For more details refer to Ref. 2).

The main assumptions in our analysis are:
1. Although the post-peak fracture process of concrete or steel spring is time dependent (according to the post-peak strain value), this effect is neglected in our analysis. The total value of the failed spring force is redistributed in the following time increment irrespective of the post-peak strain value.
2. Effects of buckling of reinforcement bars were not considered yet in the analysis as the same element represents the concrete and steel behavior.
3. In static analysis, minimum stiffness value was assumed for concrete springs after cracking. This results in having residual tension force acting at the normal springs after cracking which is redistributed in the next increment. However, this technique can not be applied in dynamic analysis cases. Assuming minimum stiffness value at the crack location affects greatly the dynamic behavior of elements after separation of structural elements. For example, rigid body motion of elements can not be followed accurately if minimum stiffness value is assumed. Hence, spring stiffness after cracking is assumed zero till the crack closure occurs.
4. After reaching 1.0% strain in concrete, compression springs are not allowed to fail.
5. Collision between elements, which are not in contact at the initial stage may occur at very large deformation level and this is not considered in the verification examples. This effect was already studied and a new method was proposed. For more details refer to Ref. 12).

## 5. VERIFICATION OF LARGE DEFORMATION DYNAMIC ANALYSIS

To verify the accuracy of the newly proposed method, case studies for large deformation analyses are performed. These cases are divided into two categories. The first one is for large deformation dynamic analysis for unstable elastic structures. These structures are supposed to have rigid body motion together with large geometrical changes.
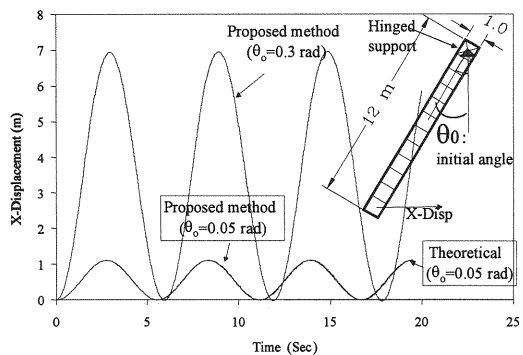


**Fig. 4** Harmonic motion of a rigid bar under own weight and initial excitation (without damping).
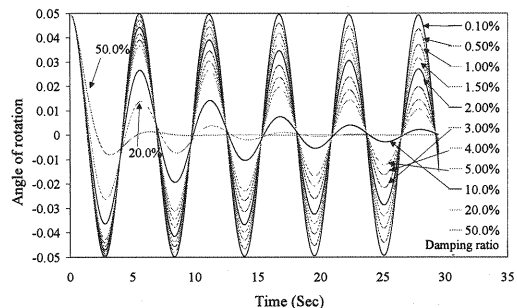


**Fig. 5** Harmonic motion of a rigid bar under own weight and initial excitation (with damping).
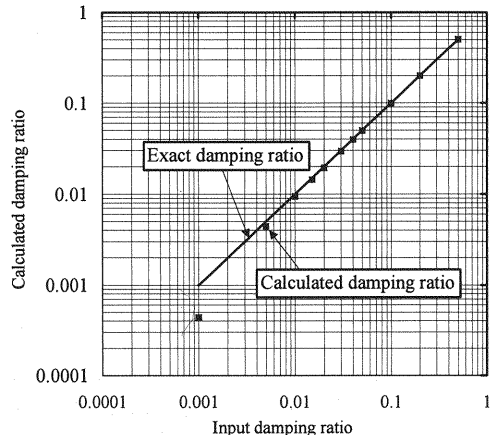


**Fig. 6** Comparison between applied and calculated damping ratios

The main objective of the first category is to compare the accuracy of the proposed technique with the theoretical results because experimental results of failed structures are not available. The other group of analyses is simulation of structures from zero loading till total collapse, and before the collision of structural elements. In all cases, the simulation time increment is 0.001 seconds.

The first case is harmonic motion of a bar due to self-weight. The bar configuration and the simulation results are shown in **Fig. 4**. Two different initial angles were used ($\theta_o$=0.05 and 0.3 rad). The result due to small angle ($\theta_o$=0.05 rad) was compared with that obtained by theory based on assumption that $Sin\ (\theta) \approx \theta$. The calculated X-displacement is almost the same as the one obtained from kinematics. When X-displacement equals zero, the rod velocity, slope to the horizontal, is always equal to the initial velocity, which is equal to zero. This indicates that there is no energy loss during the rotation of the bar. In case where $\theta_o$=0.3 rad, it is obvious that the amplitude of displacement and the oscillation period increases when the initial angle increases. This indicates that the geometrical residuals technique can simulate both the geometrical changes and rigid body motion. This analysis shows that the behavior of structural elements moving as rigid bodies after failure can be simulated.

To verify the accuracy of the proposed technique analyses using initial angle ($\theta_o$=0.05 rad) with different damping ratios are performed using the same bar shown in **Fig. 4**. **Figure 5** shows the relation between the angle θ with time. Damping ratio can also be calculated from the logarithmic decrement relationship shown in **Fig. 4** by[8] :

$$ ln\left(\frac{u_i}{u_{i+1}}\right) = \frac{2\pi\zeta}{\sqrt{1-\zeta^2}} \qquad (7) $$

where, $\zeta$ is damping ratio; $u_i$ and $u_{i+1}$, the displacement amplitude of two successive peaks.

From this equation, the applied and calculated damping ratios are compared in **Fig. 6**. Damping ratios are calculated from each time response history. From **Fig. 6**, it is clear that the applied and calculated values are very close except that when the damping ratio is less than 0.5%. For practical damping ratios, the accuracy is quite acceptable. The reason why the simulated damping ratio becomes smaller than the adopted value in very small damping case is due to underflow error during simulation.

The second case is also harmonic motion of a "L" shaped bar under its own weight. The bar configuration and results are shows in **Fig. 7**. The damping ratio used in the analysis is 4% to enable the structure to reach its stability condition. It is obvious that the bar starts oscillation around the equilibrium position. Oscillation reduces gradually and finally stops at the equilibrium position. The
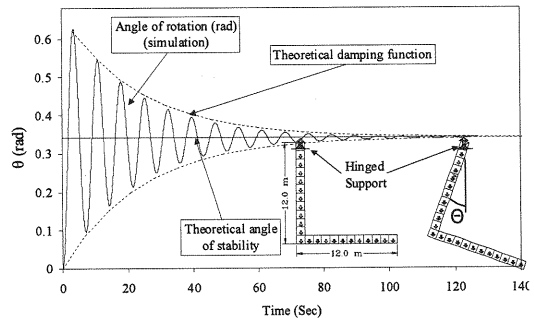


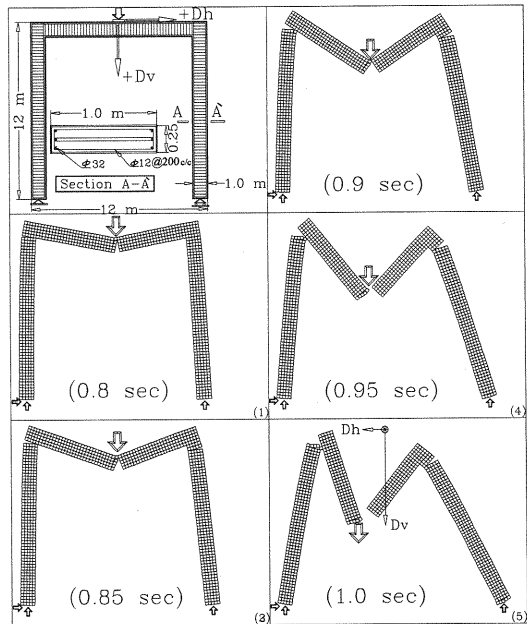**Fig. 7** Harmonic motion of a rigid "L" bar under its own weight. (Damping ratio is 4%)



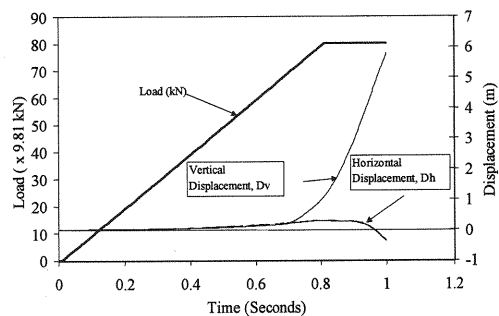**Fig. 8** Deformed shape and failure pattern of a hinged-roller RC frame



**Fig. 9** Load, vertical and horizontal displacement at the loading point vs. time

simulated angle of final stability is the same as that calculated from theory.

These two analyses show that if some part of the structure failed, the rigid body motion of this part together with the final equilibrium position can be simulated automatically. In addition, no previous knowledge about the dynamic behavior is required before the analysis.

The third example shows the time history of failure process of an RC frame. The frame is supported by hinged bearing (left) and hinged roller bearing (right). A concentrated load is applied at the center of the beam. The frame shape, dimensions, loading conditions and deformations under the applied load are shown in **Figs. 8** and **9**. The material properties are taken as follows: $\sigma_y=36$ kN/cm$^2$, $\sigma_c$ =3.5 kN/cm$^2$, $\sigma_t$ =0.21 kN/cm$^2$ and $E_c$=2000 kN/cm$^2$. Percentage of longitudinal reinforcement ratio is about 2 % of cross section. The frame is divided into 900 elements with 5 connecting springs between elements.

The failure process can be summarized as follows:
1. Cracking starts from the center of the beam because of maximum bending moment. It was verified in Ref. 2) that the failure load can be calculated accurately.
2. During loading, and before yield of reinforcement bars, cracks propagate at the center of the frame and at connections.
3. Reinforcement bars yield in the center of the beam.
4. Steel bars cut off after yield in the middle of the beam first followed by cut off in the left connection and finally the right one. The cracks at the steel cut locations dominate the behavior of the structure during failure.
5. Refering to **Fig. 9**, displacements drastically increase after 0.7 seconds because of failure of reinforcement bars. At the same time, the structure begins unstable dynamic motion.
6. Tension cracks appear at the left connection first, because of difference of supporting conditions. After midspan cracking, the beam behaves as a double cantilevers connected to unstable columns. As the loading rate is very high, crack generation at connections is faster than the rigid body motion of the failed parts.
7. Tension cracks appear at the right connection together with motion of the roller.

7. The structural members lose curvature and move as three rigid bodies in the space.

**Figure 10** shows failure pattern of a plain concrete simple beam subjected to three point bending. The beam is supported by two hinged rollers. The material properties are taken as follows: $\sigma_c$ =3.5 kN/cm$^2$, $\sigma_t$ =0.2 kN/cm$^2$ and $E_c$=2100 kN/cm$^2$. Half of the beam was simulated using 126 elements with 10 connecting springs between elements.

It can be easily seen that realistic failure behavior can be obtained. After cracking of concrete in the mid-span, the beam is separated into three parts, two beams and elements subjected to the load. The two beams rotate around the rollers till becoming vertical and then separated from the support and move as rigid bodies in the space. The elements, where the load is applied, are separated and move downward. After separation of beam segments, the rollers start inward motion. It should be emphasized that no previous knowledge of the behavior is necessary before the analysis. The crack separation location is arbitrary.

**Figure 11** shows failure mechanism of a fixed-fixed frame subjected to lateral load. The material properties are taken as follows: $\sigma_y$ =36 kN/cm$^2$, $\sigma_c$ =2.5 kN/cm$^2$, $\sigma_t$ =0.2 kN/cm$^2$ and $E_c$=2100 kN/cm$^2$. Percentage of longitudinal reinforcement ratio is about 2 % of cross section. The frame is divided to 34 elements only with 10 connecting springs between elements.

The analysis is performed till recontact between elements occurs. It is noticed that cracks mainly start from the left connections. Compression failure occurs at the right support. After having crushing of the right column support, the two columns and the attached beam moves as a rigid body. As, the effects of collision are not considered in this paper, the effects of collision with the ground elements are not presented in the current model. However, this is discussed in Ref. 12). As the number of elements is small, it took only 10 minutes using a personal computer (CPU Pentium 267 MHz) to make such analysis.

These results show that the crack initiation, crack propagation, failure of reinforcement, separation of structural members and rigid body motion of structural members after failure can be followed without any additional complications to the model.

# 6. CONCLUSIONS

In this paper, a new technique was developed by which structure behavior can be followed during loading till complete failure. Adopting geometrical residuals technique, instead of geometrical stiffness matrix, makes it easier to follow the detailed failure process including separation of structural members and rigid body motions. Moreover, the addition of the mass and inertia terms to the static stiffness matrix during solution of equations is very important to assure positive definite dynamic stiffness matrix. It means that solutions of equations of each of the elements exist even when an element and/or assembly of elements separate from the surrounding elements.

The simulation results are compared with the theoretical ones and the results showed high accuracy. The main advantages of the proposed technique are:
1. This technique is general and can be applied for any material or structural configuration, in two or three-dimensional analysis.
2. This technique does not require calculation of geometrical stiffness matrix, thus makes the analysis easier.
3. The geometrical changes of the structure during loading together with the rigid body motion of failed structural elements can be followed with reliable accuracy and without any additional complications.
4. Unlike FEM, the crack location is arbitrary. No previous knowledge about the failure process is needed before the analysis.

As the main objective of this paper is to show the wide applicability range of the proposed method, however, adopting better material models to account for proper concrete and steel behavior at high strain levels improve the accuracy of the simulation. At this stage, the main limitation of the applicability of the method is that the collision and recontact effects are not taken into account. This means that elements can separate but new element contacts are not permitted. Study on the consideration of this effect was already carried out and it will be reported in further publications.
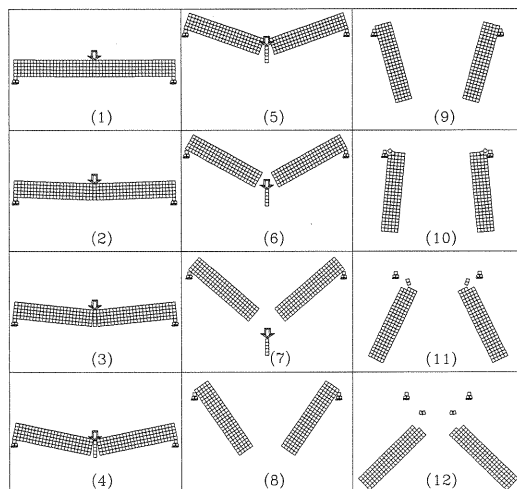


Fig. 10 Failure pattern of a plain concrete simple beam in three point bending
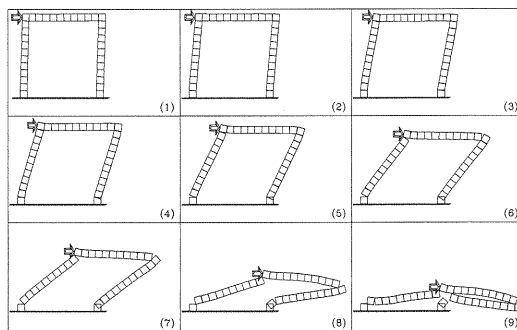


Fig. 11 Failure pattern of a RC concrete frame subjected to lateral load

## REFERENCES
1) Meguro, K. and Tagel-Din, H.: A new efficient technique for fracture analysis of structures, Bulletin of Earthquake Resistant Structure Research center No. 30, March 1997.
2) Meguro, K. and Tagel-Din, H.: Applied Element Method for structural analysis: theory and application for linear materials, Structural Eng./Earthquake Eng., JSCE. , Vol. 17, No. 1, 21s-35s, April 2000.
3) Meguro, K. and Tagel-Din, H.: Development of a new fracture analysis method with high accuracy based on discontinuous material modeling, 16th annual Conf. on Natural Disaster Reduction, Osaka, Japan, Oct. 1997.
4) Meguro, K. and Tagel-Din, H.: Simulation of buckling and post-buckling behavior of structures using applied element method, Bulletin of Earthquake Resistant Structure Research center No. 32, , pp. 125-135, March 1999.
5) Meguro, K. and Hakuno, M.: Fracture analyses of structures by the modified distinct element method, Structural Eng./Earthquake Eng., Vol. 6. No. 2, 283s-294s., Japan Society of Civil Engineers, 1989.
6) Meguro, K., Iwashita, K. and Hakuno, M.: Fracture analysis of media composed of irregularly shaped regions by the extended distinct element method, Structural Eng./Earthquake Eng., Vol. 8, No. 3, pp. 131s~142s, Japan Society of Civil Engineers, 1991.
7) William, H.: Numerical Receipes in Fortran 77, Cambridge University Press, New York, 1996.
8) Chopra, K.: Dynamics of structures, Theory and applications to earthquake engineering, Prentice Hall, 1995.
9) Walter C. and Moshe F.: Dynamics of structures, Prentice Hall, Inc., Englewood Cliffs, New Jersey, 1965.

10) Okamura, H., Maekawa, K. and Izumo, J.: Reinforced concrete plate element subjected to cyclic loading, 10th annual lecture on "FEM Analysis of Reinforced Concrete Structures", Civil Engineering Department, The University of Tokyo, 1995.

11) Ristic, D., Yamada, Y., and Iemura H.: Stress-strain based modeling of hystertic structures under earthquake induced bending and varying axial loads, Research report, No. 86-ST-01, School of Civil Engineering, Kyoto University, March, 1986.

12) Tagel-Din, H. and Meguro, K.: Analysis of a small scale RC building subjected to shaking table tests using Applied Element Method, Proceedings of the 12th World Conference on Earthquake Engineering, January 30th-February 4th, 2000.